European Journal of Echocardiography (2010) **11**, 97–108
doi:10.1093/ejechocard/jeq005

REVIEW PAPER

Automated border detection in three-dimensional echocardiography: principles and promises

K.Y. Esther Leung and Johan G. Bosch*

Thoraxcenter Biomedical Engineering, Ee2302, Erasmus Medical Center, PO Box 2040, 3000 CA Rotterdam, The Netherlands

Received 10 November 2009; accepted after revision 11 January 2010; online publish-ahead-of-print 6 February 2010

Several automated border detection approaches for three-dimensional echocardiography have been developed in recent years, allowing quantification of a range of clinically important parameters. In this review, the background and principles of these approaches and the different classes of methods are described from a practical perspective, as well as the research trends to achieve a robust method.

Keywords 3D echocardiography • Automated analysis • Border detection • Segmentation

Introduction

Motivation

Since 2008, all major ultrasound systems feature real-time three-dimensional echocardiography (RT3DE). RT3DE has been used, for example, to measure left ventricular (LV) volume and mass, to evaluate various cardiac valve problems, and to assess a spectrum of morphological cardiac disorders.[1–3] It offers possibilities for functional analysis and quantification, by avoiding the classical limitations associated with M-mode and two-dimensional echo (2DE).[4] The wealth of information in these time series of 3D data sets, however, precludes the manual tracing of borders in all these images. Therefore, automated tools for analysing these four-dimensional (4D) data sets are highly desirable. Such tools can reduce the workload and yield consistent and reproducible results for the quantification of cardiac function.

Since the breakthrough of RT3DE, several automated tools for quantitative image analysis appeared in literature and have become commercially available. In this review, we discuss their principles, provide some critical insights into their possibilities, and propose directions for future developments.

Development of real-time three-dimensional echocardiography and automated analysis

Initially, dynamic 3D echocardiography was hampered by slow acquisition and disappointing image quality. Nevertheless, some approaches for automated analysis were proposed, especially on 3D transoesophageal (TEE) data sets[5] acquired by ECG-triggered image plane rotation. Between 1990 and 1995, the first real-time 3D imaging systems using sparse-array matrix transducers were developed at Duke University, resulting in the Volumetrics RT3D system, which sparked several automated methods for LV quantification.[6,7] The breakthrough of RT3DE came around 2002 with the Philips Sonos 7500 system and the X4 matrix transducer, providing much better image quality. Shortly thereafter, 3D analysis approaches became available (TomTec 4D LV-Analysis, version 1,[8] and Philips QLab 3DQ-Advanced[9]). Meanwhile, other vendors have introduced RT3DE systems [GE-Vingmed Vivid 7 with 3V probe (2004), Siemens-Acuson Sc2000 with 4Z1c probe (2008), and Toshiba Artida with PST-25SX probe and 3D wall tracking (2008)]. TomTec Imaging Systems pioneered many of the tools for 3D acquisition and analysis in the early days, including those on several manufacturers' analysis platforms. 3D image acquisition technology is advancing at a rapid pace; Philips expanded 3D functionality with its iE33 platform, the X3-1 transducer, the X7-2 paediatric transducer, and the first matrix TEE transducer (X7-2t). GE-Vingmed has introduced a new platform (Vivid E9) with improved 3D functionality.

Promises and challenges

Real-time three-dimensional echocardiography vs. two-dimensional echo

The clinical advantages and practical use of RT3DE have been presented in a number of recent reviews.[2–4] RT3DE is also especially

* Corresponding author. Tel: +31 10 7038088, Email: j.bosch@erasmusmc.nl

important for *quantification* of LV volumes, LV mass, segmental wall motion and synchrony, etc. Because all structures can be seen in context, a consistent outlining of the whole endocardial surface is usually possible. There is no underestimation of volume due to foreshortening or shape assumptions, like in 2DE. However, the image quality, frame rate, and resolution of RT3DE are lower and artefacts such as shadowing are more common than in 2DE. The amount of image information is enormous, making manual analysis cumbersome.

Challenges in real-time three-dimensional echocardiography analysis

Quantitative analysis of RT3DE is generally more challenging than, for example, of computed tomography (CT) or magnetic resonance (MR), for multiple reasons.

(i) Parts of the anatomy are not imaged, due to dropouts (for structures parallel to the ultrasound beam), shadowing (behind acoustically obstructive structures such as ribs and lungs), and scan sector limitations. Because of the relatively large footprint of 3D transducers, shadowing is often a problem.
(ii) Artefacts caused by side lobes, reverberations, clutter, etc. are common. Most artefacts increase with reduced ultrasound penetration, which is frequent in obese or older patients.
(iii) Pixel intensity does not directly reflect any physical property of the tissue. Ultrasound images are formed by sound reflection and scattering, resulting in the typical ultrasound *speckle patterns*. Different tissues and blood are often not distinguished by intensity, but only by subtle differences in (moving) speckle patterns. The exact interface between blood and tissue is not always clear.
(iv) The sequential scanning of ultrasound lines merges information from different time moments into one image. For quickly moving structures, this leads to spatial distortion and sharp transitions between 'older' and 'newer' image parts. In RT3DE, this is particularly prominent where subvolumes from different heartbeats are stitched together to image the complete LV.

Border delineation is needed for quantification

To derive useful clinical parameters from RT3DE, one should outline the structures of interest, e.g. the endocardial border delineating the 3D lumen. Classically, this is done manually. In a standard biplane volume analysis, there are just a few borders to draw. The earliest 3D echo analysis software either required manual delineations in many cross-sectional views (TomTec Echoview), which were then spatially interpolated to a single 3D volume, or used manual delineation in two perpendicular views, after which the standard biplane Simpson's rule is applied (Philips QLab 3DQ). A typical complete volumetric analysis would require internally consistent manual drawing of hundreds of borders (10–20 borders in 15–30 3D images). Therefore, for an objective, reproducible quantification and a practical workflow, an automated analysis is highly desirable.

Image processing for real-time three-dimensional echocardiography

Computer analysis of images: the image interpretation pyramid

Automated image analysis or *image processing* involves complicated computer processing that mimics the human visual interpretation system. Although we humans perform visual perception constantly with ease, we do not realize *how* we actually do it. [A look at some of the well-known optical illusions (http://www.michaelbach.de/ot/) demonstrates how much hidden interpretation is going on in our 'infallible' vision system.] To clarify the possibilities and limitations, we will use the metaphor of the *image interpretation pyramid* (*Figure 1*). We can distinguish multiple levels in how we derive meaning from the light that reaches our eyes. At the bottom (level 0) resides the basic information that our retina cells provide: light intensity and colour, comparable to the pixels in a digital image. At level 1, image *features* are located: patches with similar information, edges where brightness varies, corners, motion, etc. At level 2, such features aggregate into *patterns* or *objects* with some relation to our world. Higher up (level 3), we have a *scene* with an interaction of objects. At the top (level 4), some meaningful *interpretation* is produced, e.g. 'a wall motion abnormality that is likely caused by a stenosis in the left anterior descending coronary'. The levels represent increasing abstraction as well as data reduction. In medical image interpretation, knowledge on anatomy and pathology is contained at levels 3 and 4. The knowledge on the imaging modality resides at levels 1 and 2—i.e. the way structures and artefacts appear in an ultrasound image.

For interpretation, we employ a huge amount of specialized knowledge at each level, by fitting 'models' of what we know and need to the data, and disposing of the 'uninteresting' information. A *model* signifies *prior knowledge* of what is meaningful or expected. However, this is not a simple bottom-up process, and interaction between levels often occurs, to deal with conflicting or ambiguous possibilities, to fill in missing information, etc. With the current state of technology, only limited aspects of the human visual interpretation can be mimicked in a computer and only relatively simple models are employed in automated image analysis.

Overview of three-dimensional segmentation methods

A wide range of image processing approaches for LV quantification in RT3DE have been proposed. These are generally identified as *segmentation*, *border detection*, *object detection*, *tracking*, *registration*, or *classification*. *Segmentation* is defined as dividing an image into different objects or classes (such as tissue and blood), or as finding their borders (*border detection*). In *object detection*, the presence and position of certain structures (such as a valve) is determined. It is often linked to *classification*, an approach where pixels or parts of images are given a label based on some decision scheme. In *tracking*, the

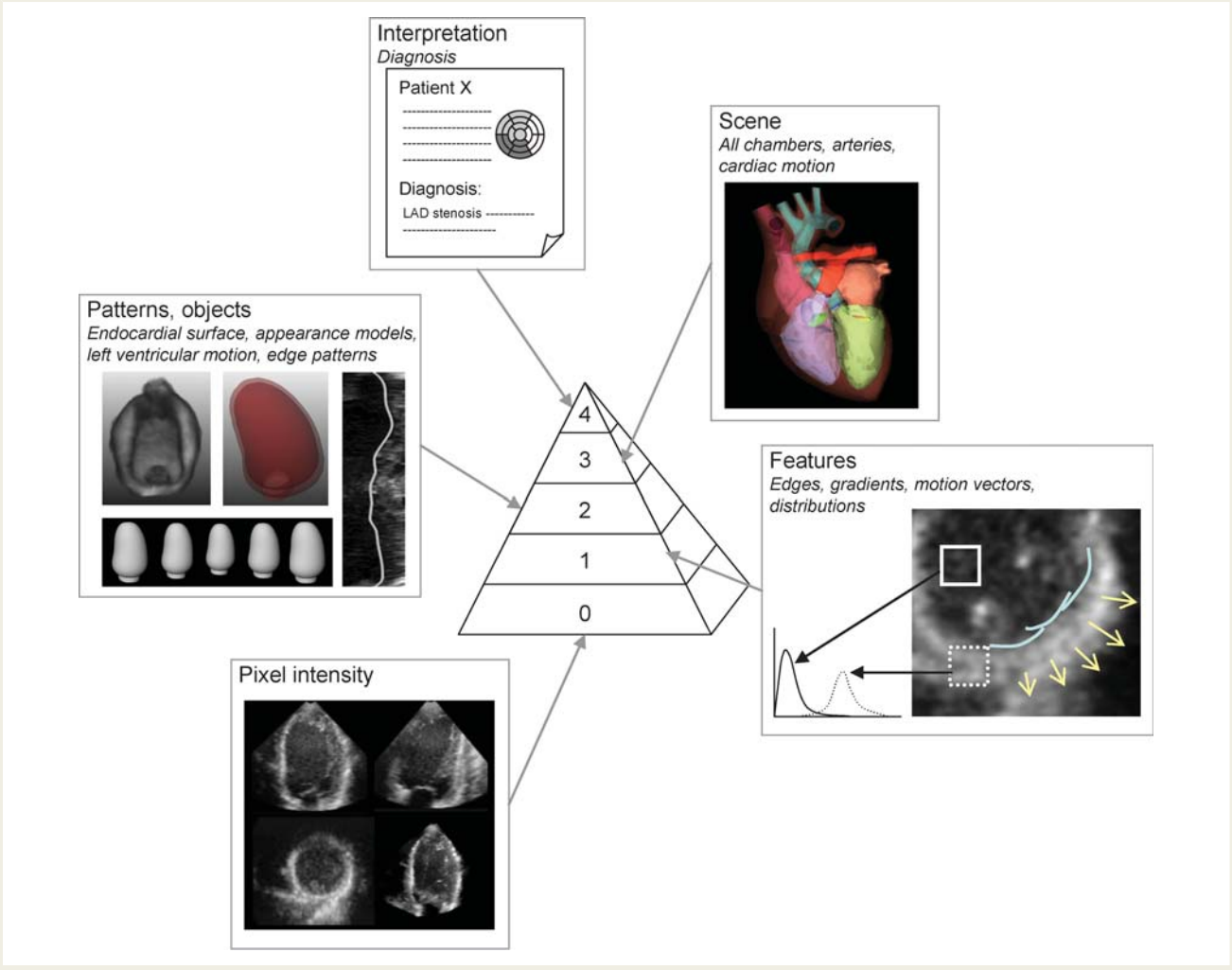

Figure 1 The image interpretation pyramid.

position of a point or structure in an image is followed over time. In *registration*, the deformation between images (such as consecutive images in time, or follow-up images vs. baseline) is determined, so that the displacement is known for any point.

Although the distinctions are not strict, these techniques provide different solutions for related problems. For example, strain estimation may use registration or tracking, and a fully automated localization of the LV may use both classification and segmentation.

In this review, we will concentrate on finding ventricular borders in non-contrast-enhanced echocardiograms, for single or time series of 3D images. Most papers focus on endocardial border detection; a few also discuss the epicardium (*Table 1*). In principle, most automated methods are suitable for both. However, the epicardium is harder to detect since it is usually less visible and has a varying appearance in different segments. Epicardial border detection is usually assisted by the endocardial border detection, e.g. by assuming typical distances between both borders.

The methods mostly operate on B-mode data [envelope of the radiofrequency (RF) signal]. Although the phase information contained in the RF signal is very important for detecting subtle cardiac deformation in strain analysis,[10] it may be less beneficial in detecting tissue boundaries. However, both approaches may benefit from each other. In contrast to most strain analysis methods, 3D segmentation methods operate typically in the Cartesian 3D space rather than in the polar (scanline) domain, since generally some kind of 3D geometrical assumption of the LV is employed, which is cumbersome in the polar domain.

For obvious reasons, we cannot give a detailed overview of all available methods; the most important ones are summarized in *Table 1*. For more in-depth technical details, we refer to the excellent overview by Noble and Boukerroui.[11]

Geometrical models

The most common border detection approaches are based on *geometrical models*. The border is represented as a curved surface which separates the lumen from the cardiac wall. This surface is influenced by geometrical constraints, e.g. the surface must resemble a certain shape (such as an ellipsoid), it must be 'smooth' in some respect, etc.

Table 1 Automated border detection methods

Category	Subcategory	Method
Geometrical models	Deformable models via energy function optimization	2D + T: TomTec 4D LV-Analysis, version 1,[8,17,55,56,63–69] also for epicardial borders[70] 3D + T: TomTec 4D LV-Analysis, version 2,[17,18,57,71,72] for right ventricle,[19,73–76] QLab 3DQ Advanced: LV endocardium,[21,54,56,58,71,77,78] also for epicardium,[70,79] left atrium[80,81] 4D LVQ in GE EchoPAC[22] guided by registration,[13] congenital heart disease,[15] epicardial and endocardial,[14,16,24,82] other academic papers[7,9,12]
	Other optimization types	Dynamic programming and pattern matching,[83] geometrical model for tracking[62,84]
Shape-free methods	Clustering	Clustering of pixels: Gaussian distribution with interactive thresholding,[23] Rayleigh distribution,[24] multiscale intensity-based features,[25] phase-based features[26,27]
	Level sets	For LV,[29,32] also for epicardial borders,[85] multi-scale level sets,[30,31] LV + RV[28]
Statistical modelling	Active shape models	Multislice shape model,[34,36] optimization via Kalman filtering[35]
	Active appearance models	3D data,[38,39] triplane data[37]
Classification	Pixel/feature	Edge segments,[40] surface[86]
	Entire image	Marginal space learning, probabilistic boosting tree[41,42]
Tracking	Registration	Global spatial transform,[13,82] local spatial transform[46,47]
	Speckle tracking	Strain estimation: Toshiba Artida,[50–52] block matching,[48,49,53,87] optical flow,[48] combined with statistical motion patterns[44,45]

To find the borders, an initial guess of the surface is placed on the image, either automatically or interactively. This surface is then *optimized* or 'deformed' to a new position, guided by image features (e.g. edges), which are associated with the true border. This is often done *iteratively*: the features close to the surface are used to *repetitively* update the surface, until it does not change significantly anymore.

Most methods use energy-based optimization. These approaches are known as *deformable models*, balloons, snakes, and active contours.[7,9,12–16] A mathematical 'energy' function is defined, which consists of an 'external' and an 'internal' component. The external component is determined by the image features, and the internal component limits the area and curvature of the surface to ensure smoothness. The total function is then optimized iteratively. These methods may differ in the mathematical representation of the contours, the type of image features, and the way of obtaining the initial guess of the surface.

One of the earliest examples is the TomTec 4D LV-Analysis (version 1).[8,17] The mitral valve annulus is manually annotated in eight long-axis cross-sections, in end-diastole (ED) and end-systole (ES). An ellipse is placed close to the annotated points as the initial guess. The borders in these cross-sections are then detected using intensity-based features close to the ellipse. The borders are represented by a spline (a mathematical description of a smooth curve). These 2D borders are then spatially interpolated to a 3D surface. In a newer version of this software (TomTec 4D LV-Analysis, version 2; *Figure 2*), manually traced borders in three views (the four-chamber view, and views at 60° and 120° rotation) in ED and ES are used as initialization. A 3D *spatio-temporal* deformable model is then applied,[17,18] which ensures a smooth surface in time and space. The TomTec 4D RV-Function software uses essentially the same approach in the right ventricle (RV). In this case, the method is initialized by manual delineation of the borders in two perpendicular long-axis views.[19]

The Philips QLab 3DQ-Advanced software[20,21] (*Figure 3*) uses five manually placed points (four on the mitral valve annulus and one on the apex) in ED and ES as initialization. This method also uses a *coarse-to-fine* (*multiscale*) scheme, gradually going from global changes in position of the surface (driven by global rotations, translation, scaling, and shear) to local refinements for each surface segment.[9]

Recently, GE introduced the 4D LVQ tool in the EchoPAC software[22] (*Figure 4*), which uses 18 manually placed points as initialization (mitral valve annulus and apex on three apical views, in ED and ES).

Geometrical modelling uses multiple levels of the image pyramid, employing a geometrical surface (level 2), driven by image features (level 1) and intensities (level 0). They are quite flexible, allowing a wide variety of shapes. Therefore, they are especially useful if the borders are expected to vary a lot, e.g. if congenital heart disease is present.[15] However, it is difficult to achieve the right balance between surfaces which are too smooth (too indistinctive for all pathological variabilities) and surfaces which are entirely implausible.

Shape-free methods

Shape-free methods rely heavily on image pixels and features (levels 0 and 1 of the image pyramid). Few assumptions are made on the shape of the border; arbitrary shapes are allowed.

Clustering

Clustering techniques are often used to categorize image pixels into distinct groups, based on image features. For example, one can categorize each pixel into myocardial tissue or blood, based on its

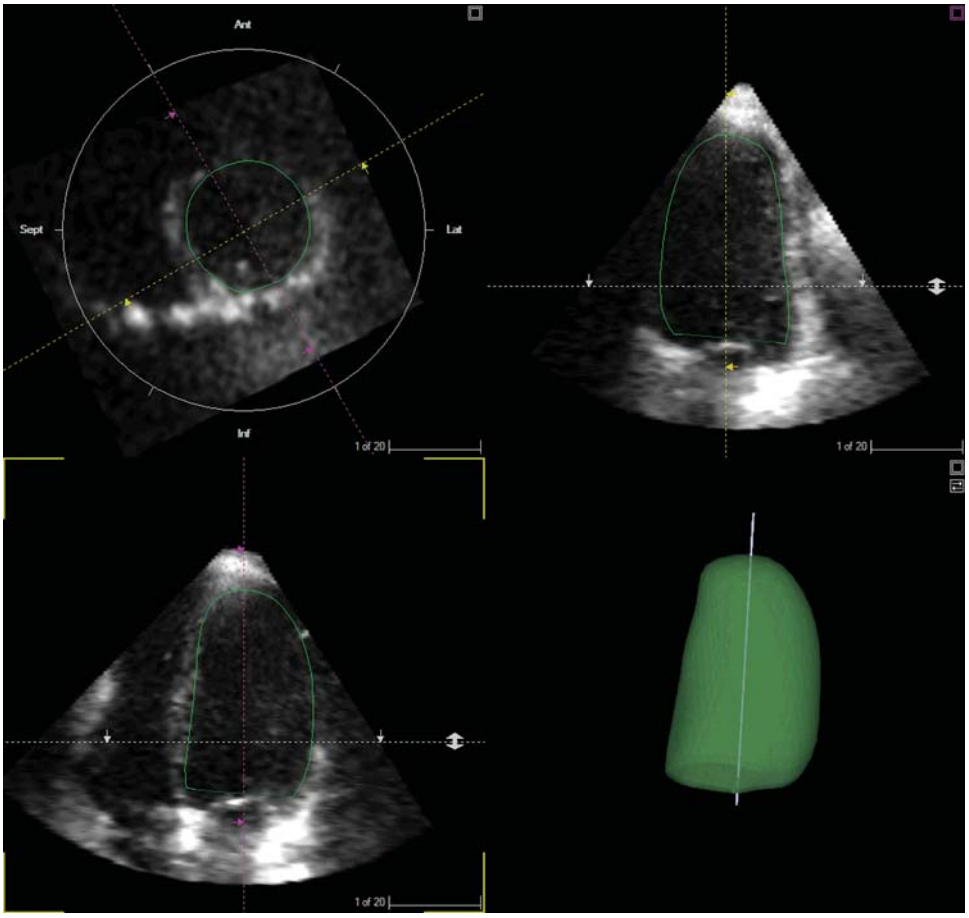

Figure 2 TomTec 4D LV-Analysis. The border detection method is based on geometrical modelling using spatio-temporal splines. Courtesy of TomTec Imaging Systems GmbH (Unterschleissheim, Germany).

intensity.[23] The underlying assumption is that the intensity distribution in tissue (high intensities) differs from the distribution in blood (low intensities). Methods may use different distributions; e.g. the Gaussian[23] and the Rayleigh distributions (which is more tailored to ultrasound images).[24] Besides intensities, other types of features may be used (e.g. features based on phase[25,26]). The segmented object may not necessarily be in one piece, thus allowing maximum freedom in shape and topology. However, given the peculiarities in ultrasound imaging, it is often necessary to incorporate higher-level knowledge. Therefore, clustering is often integrated into modelling methods (e.g. geometrical models and motion models[27]), to give a more stable detection.

Level sets

The *level sets*[6,28–32] approach is quite similar to energy-based deformable models. However, with level sets, the curved surface is defined by a different deformation equation such that the shape of the borders is much less restricted. (Theoretically speaking, energy-based deformable models are explicit mathematical formulations of level sets and are therefore closely related; in practice, however, level sets give much more flexible shapes.) The detected border may consist of multiple disconnected surfaces. This is potentially useful in pathological cases (e.g. ventricular septal defects) or for segmenting the whole-blood pool in all four chambers simultaneously. Obviously, due to the shape-free nature, the method is sensitive to shadowing and dropouts.

Population-based statistical models

Statistical modelling methods model the statistical variations in actual patient data from large sets of images with expert-drawn borders. Statistical modelling condenses patient variability into a relatively simple mathematical model which has only a few parameters, but with very strong descriptive power. The patient variability is expressed as an 'average' and several 'typical modes of variation' (i.e. *eigenvariations*), obtained using principal component analysis. Both the borders (*shape model*) and the image intensities (*texture model*) can be represented in this way. By choosing different weights (i.e. parameters) for each eigenvariation, a wide range of shapes and images can be synthesized, covering all patient variation. As it models the variability from real data, the method deals with knowledge at pyramid level 2.

By explicitly learning variations from real examples, the method finds only plausible results, even if they are very complex. It captures the expert's definition of proper border definitions (which

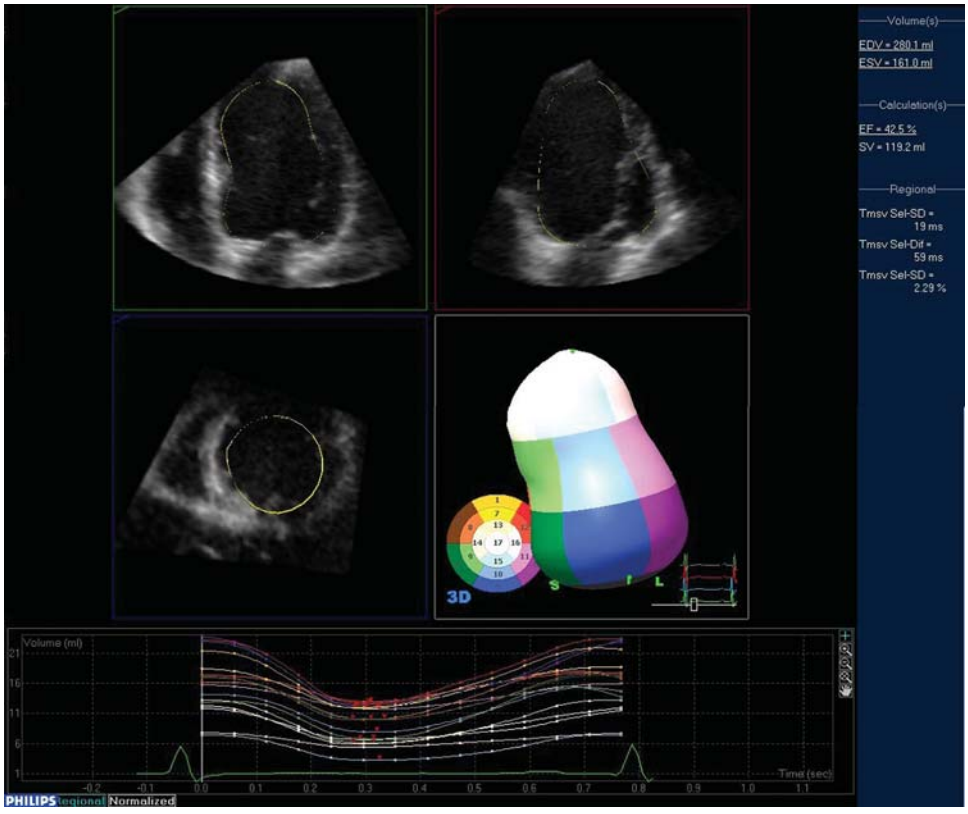

Figure 3 Philips QLab 3DQ-Advanced software. The method is initialized using five manually placed points on the apex and mitral valve annulus, after which a deformable model is applied. Courtesy of Philips Medical Systems (Andover, MA, USA).

may not necessarily be the 'brightest' edge in the image), even in the presence of typical ultrasound artefacts. It can also be extended to model all cardiac phases simultaneously.[33] However, a large database is needed which is representative of the expected variations, including pathological cases. Also, the accuracy depends directly on the quality and consistency of the expert-drawn borders.

Active shape models

Active shape models use mainly a shape model for border detection.[34–36] First, the average shape is placed on the image. The parameters of the shape model are then found iteratively: similar to the geometrical models, the local image features drive the shape model to the actual borders, but here, the statistical shape model is the geometrical constraint. Only 'plausible' shapes are found in this way.

Active appearance models

Active appearance models use a somewhat different border detection strategy, by taking both texture and shape variability into account.[37–39] An *appearance model* is obtained by applying principal component analysis on the combination of the shape and texture models (*Figure 5*). The model is then adapted to match the image iteratively: the difference between the model-synthesized image and the real image determines the next best estimate of the appearance model. Since the active appearance model uses a model of the texture, it uses more expert knowledge than the active shape method. This is especially useful in regions which contain typical artefacts. However, this requires that the texture model can represent all expected variations, and more examples are needed.

Classification using expert-created databases

Classification techniques use expert-created databases for automated grouping and recognition of many types of objects, such as fingerprints, handwritten text, speech, etc. Owing to its versatility, classification can be adapted to all levels of the image pyramid, for categorizing image pixels (level 0) and features (level 1), and even for image interpretation (level 4).

Experts distinguish different groups or regions in a large database of example data. This database is used to learn a division between classes of objects, given their features. The feature distribution of both classes must be as distinct as possible, by selecting the most descriptive features, the appropriate distributions, and a suitable mathematical method to learn the division.

In the past, classification was mostly applied to divide the image on a very local basis: classifying each pixel (blood or cardiac tissue) or small sets of features (edge or no edge[40]). Recent methods use all features in the image to detect the entire LV border.[41] Parts of an image are classified by placing boxes of different sizes on the

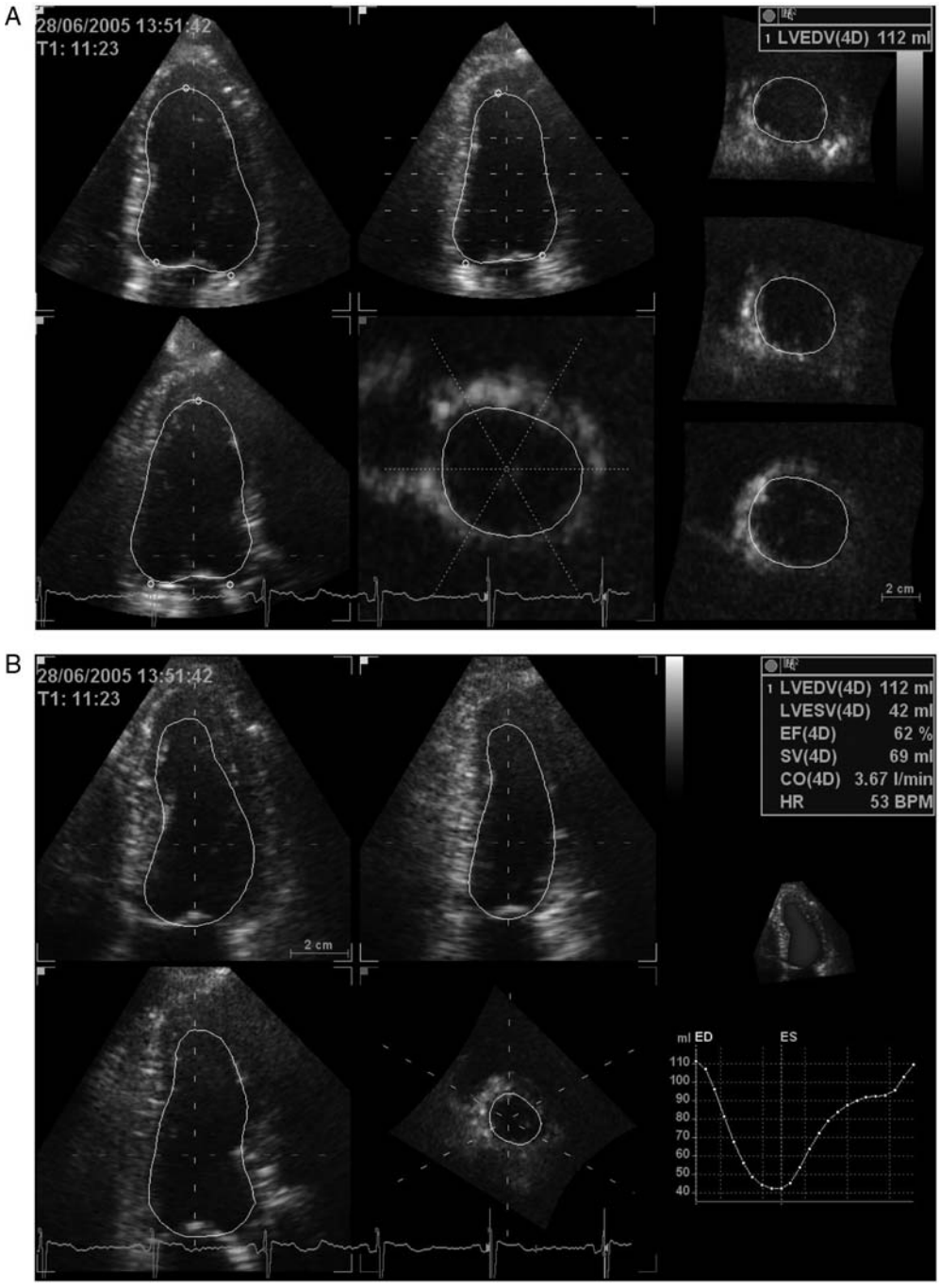

Figure 4 Left ventricular surface detection using 4D LVQ in EchoPAC software. (*A*) Borders are initialized by manual annotation of mitral valve annulus and apex in the standard apical views. Three extra SAX views were used to further verify the detected surface. (*B*) The complete four-dimensional surface detection at end-systole with time–volume curve. Courtesy of J. Hansegård (GE Vingmed Ultrasound, Horten, Norway).

image in different positions. The classifier determines for each box whether it contains a centred LV. The strength of this method lies in the use of a classifier (a so-called probabilistic boosting tree), which automatically selects a powerful combination of simple features. In practice, the classification algorithm follows a coarse-to-fine scheme (*marginal space learning*). This method was used to detect anatomical planes (four-chamber, two-chamber, and short-axis cross-sections)[42] and the 3D borders in ED.[41] Siemens is in the process of integrating these methods into the Acuson sc2000 system.[43]

This promising technique uses expert knowledge for border detection, by learning from real patient data. Also, the detection

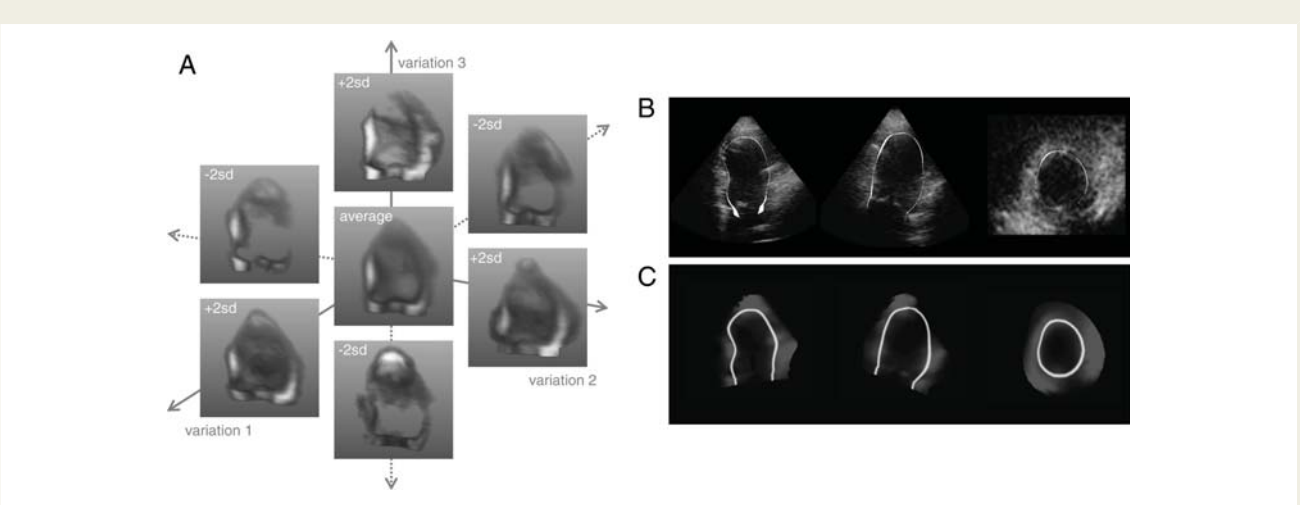

Figure 5 (*A*) Three-dimensional appearance model of the left ventricle, showing the average appearance and the main variations. (*B*) Four-chamber, two-chamber, and short-axis cross-sections of a three-dimensional image with manually delineated borders. (*C*) The corresponding image and borders, synthesized by the appearance model.

can be very fast. However, many consistently delineated example images are needed to build an accurate classifier, considerably more than for statistical models (around 4000 examples[43]).

Intensity-based tracking

As *tracking* involves the estimation of motion, it is strictly speaking not a border detection method; rather, it can be used to *propagate* borders throughout the cardiac cycle, by applying the estimated motion frame-by-frame to the borders in the first frame.

Most often, tracking uses only image intensities (pyramid level 0) to guide the border detection. If two images are very similar, the motion can be estimated quite accurately. However, tracking is sensitive to image noise and artefacts. Therefore, information from higher levels of the image pyramid, such as knowledge of cardiac motion patterns,[44,45] are often effective.

Registration

Registration methods find the spatial correspondence between images. This is estimated by iteratively optimizing a similarity measure between two images. This measure is often based on local image intensities (e.g. sum-of-squared differences, cross-correlation), or on overall intensity distributions, such as mutual information. The latter, less strict criterion makes it especially useful in registering images of different image modalities. The spatial correspondence is expressed by a spatial transform: global transforms such as rotation, translation, scaling, and shear;[13] or more complex, local transforms, such as deforming a spline grid.[46,47] The complexity of the transform influences the precision of the motion pattern, but also the computation time. Usually, many iterative steps are needed, which makes registration methods relatively slow. Therefore, registration is often applied in a coarse-to-fine manner, by increasing the image resolution and the complexity of the transform in each stage.

Speckle tracking

Speckle tracking finds corresponding speckle patterns in different frames. The most popular speckle-tracking methods are based on *block matching* or *optical flow*; in most cases, a rough estimate is first found using block matching, which is then refined using optical flow.[48] Both methods can be implemented in a coarse-to-fine scheme.[49] Recently, Toshiba has introduced the Artida system, which has a 3D speckle-tracking method[50–52] (*Figure 6*).

Block matching looks for similar speckle patterns in two images by transforming part of an image to match another image.[53] The transform corresponding with a maximal similarity measure (e.g. cross-correlation) is the estimated motion. The transform, e.g. translation and rotation, is applied in fixed intervals. Therefore, the computation time is limited, but the accuracy of the motion estimation is also limited to these intervals.

Optical flow uses image gradients to estimate motion. The motion is found by solving a mathematical equation that relates the spatial and temporal image gradient to the motion. The most common methods either incorporate global constraints (smoothness of the motion in the entire image) or local constraints (constant motion within a small image region). If applied to cardiac images, statistical models of the cardiac motion may be used as a constraint instead.[45] Since optical flow allows a seamless integration of scaling and shearing, the method can (theoretically) also be used to estimate subtle motion patterns, to easily derive parameters such as strain and strain rate.

Discussion

All approaches described above have been evaluated with positive outcome. Especially the commercial systems that have been available for some time (Philips QLab and TomTec 4D LV) have been used in many studies (*Table 1*). Here, we will discuss some aspects and comparisons between the different approaches.

Figure 6 Strain estimation based on speckle tracking in the Toshiba Artida system. (Top) Peak circumferential strain at end-systole. (Bottom) Torsion at early diastole. Courtesy of W. Gorissen (Toshiba Medical Systems Europe, Zoetermeer, The Netherlands).

Ground truth for borders and quantitative parameters

Validation of automated border detection in medical images is not trivial. An accurate ground truth for border delineation and volume measurement is absent.

First of all, direct *in vivo* assessment of borders or volumes in humans is impossible. *Ex vivo* materials, animal experiments, casts, phantoms, etc. are regularly used for fundamental validation; these can be controlled well, but rarely resemble the human *in vivo* situation.

Secondly, RT3DE borders and volumes are often compared with other imaging modalities like MR imaging (MRI) or CT, but these give a different impression of the same anatomy, due to the underlying physical principles of imaging. Especially, the heavy trabeculations on the LV endocardial wall induce differences between ultrasound and MRI.[54] Several studies have shown that it is possible to get good correspondence between volumes derived from MR and RT3DE,[8,17,55–57] provided that adapted tracing conventions are applied. Reconsideration of the classical tracing conventions is required, using the insights of such studies.[54]

Thirdly, the automated borders can be compared with borders drawn by experts. However, considerable variability will exist between the borders of different experts, between different institutions, and even within one expert, if an analysis is repeated. Barely noticeable variations can cause significant changes in volume.[54] Also, interpretation consensus will decrease for images of lower quality or clinically more difficult cases. In practice, an automated method is considered acceptable if it is within a predetermined range of expert variability.

Comparison of different approaches

It is even more difficult to determine which method performs best, or under which circumstances, methods succeed or fail. Especially, image quality plays an important role in the quality of RT3DE analysis. Comparing the numbers in different evaluation studies is meaningless. The analysis circumstances, image quality, and patient data may vary widely. Few studies compare methods on the same set of data.[17,22,56,58] Usually, a single set of manually drawn borders or analyses on MRI or CT are used as 'reference standards', with limitations as sketched above. The general conclusion is often that the results do not differ significantly, and that one method is superior in terms of reduced user interaction, processing time or observer variability. Of course, these are important secondary issues, but which method delivers the most accurate results remains unanswered.

Need for well-validated data sets

In the light of the above, a large, standardized database is required covering a range of image quality, of pathological and normal cases with borders well validated by multiple observers. Such a database is ideal for the objective comparison of methods or consecutive versions of algorithms, to determine their limitations under varying circumstances and for optimization purposes. Similar databases exist in other domains, such as for brain MR (see http://www.cma.mgh.harvard.edu/ibsr), chest radiographs, and liver segmentation in CT images.[59] These databases may considerably boost the improvement of methods, e.g. via large-scale competitions.[59]

Fully automated vs. interactive methods

From the viewpoint of logistics and user effort, fully automated analysis would be highly attractive, by eliminating user variability and allowing unsupervised and possibly on-line quantification. In principle, it might even allow automated patient monitoring. However, monitoring applications pose very severe requirements on sensitivity and specificity. Given the highly varying image quality, the complex nature of the ultrasound images, and the considerable amount of artefacts, *unsupervised* analysis seems currently far out of reach.

The clinician has the obligation and should have the possibilities to verify and correct automated quantifications. Also, good methods should ensure spatial and temporal consistency after correction, and should limit the effect of initialization and correction on observer variability. Many of the current methods could be improved in this respect.

Future developments

Developments in 3D ultrasound segmentation have resulted in multiple promising methods of which some have proven their practical value. It is clear that there are many possible improvements and extensions.

Image quality

First of all, accuracy of 3D analyses is still seriously limited by the 3D image quality and severe artefacts. Further improvements in 3D image quality will directly improve outcome of quantification. It can be expected that image quality and resolution of RT3DE will improve towards the quality of 2D ultrasound, since this is mainly determined by instrumentation electronics and signal processing capabilities. Higher frame rates will improve the accuracy of ejection fraction and regional wall motion synchronicity measures.

However, image quality and artefacts will always remain an issue in ultrasound. Actually, a good method should estimate the image quality and adapt its approach. Therefore, an internal estimate of the reliability and probability of its outcome is an essential aspect of a well-behaved automated method.

More prior knowledge on scene and anatomic variability

The current segmentation approaches are mostly limited to a single object: the LV endocardial surface. For RV and LA, some experimental approaches are appearing (*Table 1*). Moreover, all methods require manual initialization. They operate mainly on abstraction levels 2 and 3 of the pyramid (features and objects); for more abstract prior knowledge, they rely on human intervention. Automated analyses can still be significantly improved by using information at the higher abstraction levels. Population modelling and high-level classification are being developed that incorporate knowledge of the higher abstraction levels. These techniques may allow less user interaction and stay closer to physiologically probable solutions. Interpretation of a *multiobject scene* (endocardium, epicardium, valves, atria, and vessels) will result in more and novel parameters and can also improve detection accuracy. Such 'complete' heart models have already shown their value in CT.[60] Both academic and commercial developments are working in these directions.

Integration of contrast, Doppler, and three-dimensional strain

Relatively, little work has been done on border detection of contrast-enhanced RT3DE,[36,45] and the integration of Doppler and strain information with border detection.[61] These terrains may greatly extend the range of possible quantifications and improve detection accuracy.

Real-time analysis

Ultimately, real-time analysis should provide direct quantification during acquisition, allowing many new applications of RT3DE. Some promising work takes place in this direction.[43,62] The optimal tool for RT3DE analysis in our view would indeed be a fully automated real-time approach, provided that it is combined with effective human supervision and smart interactive correction as well as solid reliability estimates.

Conclusion

Much has been achieved recently in the field of automated analysis of RT3DE, and much more is still to come. More automated initialization, reliability feedback, and smart interactive correction tools are expected. A standardized database of patient data might allow improvement and quality assessment of different methods.

Current approaches still make limited use of available prior knowledge. Powerful population-based multiobject models are promising in this respect. Fully automated real-time analyses will allow new applications for RT3DE. Such next-generation automated analyses will directly provide superior quantitative information and boost the role of 3D echocardiography in clinical practice.

Conflict of interest: K.Y.E Leung's PhD project was partially supported by TomTec Imaging Systems GmbH and Philips Medical Systems.

Funding

K.Y.E. Leung was supported by the Dutch Technology Foundation STW (grant 6666), applied science division of NWO and the Technology Program of the Ministry of Economic Affairs.

References

1. Lang RM, Mor-Avi V, Sugeng L, Nieman PS, Sahn DJ. Three-dimensional echocardiography: the benefits of the additional dimension. *J Am Coll Cardiol* 2006;**48**:2053–69.
2. Yang HS, Bansal RC, Mookadam F, Khandheria BK, Tajik AJ, Chandrasekaran K. Practical guide for three-dimensional transthoracic echocardiography using a fully sampled matrix array transducer. *J Am Soc Echocardiogr* 2008;**21**:979–89.
3. Mor-Avi V, Sugeng L, Lang RM. Real-time 3-dimensional echocardiography: an integral component of the routine echocardiographic examination in adult patients? *Circulation* 2009;**119**:314–29.
4. Monaghan MJ. Role of real time 3D echocardiography in evaluating the left ventricle. *Heart* 2006;**92**:131–6.
5. Roelandt JRTC, ten Cate FJ, Vletter WB, Taams MA. Ultrasonic dynamic three-dimensional visualization of the heart with a multiplane transesophageal imaging transducer. *J Am Soc Echocardiogr* 1994;**7**:217–29.
6. Corsi C, Borsari M, Consegnati F, Sarti A, Lamberti C, Travaglini A *et al.* Left ventricular endocardial surface detection based on real-time 3D echocardiographic data. *Eur J Ultrasound* 2001;**13**:41–51.
7. Angelini ED, Laine AF, Takuma S, Holmes JW, Homma S. LV volume quantification via spatiotemporal analysis of real-time 3D echocardiography. *IEEE Trans Med Imaging* 2001;**20**:457–69.
8. Kühl HP, Schreckenberg M, Rulands D, Katoh M, Schäfer W, Schummers G *et al.* High-resolution transthoracic real-time three-dimensional echocardiography: quantitation of cardiac volumes and function using semi-automatic border detection and comparison with cardiac magnetic resonance imaging. *J Am Coll Cardiol* 2004;**43**:2083–90.
9. Gérard O, Billon AC, Rouet J-M, Jacob M, Fradkin M, Allouche C. Efficient model-based quantification of left ventricular function in 3-D echocardiography. *IEEE Trans Med Imaging* 2002;**21**:1059–68.
10. D'Hooge J, Heimdal A, Jamal F, Kukulski T, Bijnens B, Rademakers F *et al.* Regional strain and strain rate measurements by cardiac ultrasound: principles, implementation and limitations. *Eur J Echocardiogr* 2000;**1**:154–70.
11. Noble JA, Boukerroui D. Ultrasound image segmentation: a survey. *IEEE Trans Med Imaging* 2006;**25**:987–1010.
12. Montagnat J, Sermesant M, Delingette H, Malandain G, Ayache N. Anisotropic filtering for model-based segmentation of 4D cylindrical echocardiographic images. *Pattern Recogn Lett* 2003;**24**:815–28.

13. Zagrodsky V, Walimbe V, Castro-Pareja CR, Qin JX, Song JM, Shekhar R. Registration-assisted segmentation of real-time 3-D echocardiographic data using deformable models. *IEEE Trans Med Imaging* 2005;**24**:1089–99.
14. Walimbe V, Zagrodsky V, Shekhar R. Fully automatic segmentation of left ventricular myocardium in real-time three-dimensional echocardiography. *Proc SPIE Med Imaging* 2006;**6144**:61444H.
15. Nillesen MM, Lopata RGP, Gerrits IH, Kapusta L, Huisman HJ, Thijssen JM *et al.* Segmentation of the heart muscle in 3-D pediatric echocardiographic images. *Ultrasound Med Biol* 2007;**33**:1453.
16. Garson CD, Li B, Acton ST, Hossack JA. Guiding automated left ventricular chamber segmentation in cardiac imaging using the concept of conserved myocardial volume. *Comput Med Imaging Graph* 2008;**32**:321–30.
17. Soliman OI, Krenning BJ, Geleijnse ML, Nemes A, Bosch JG, van Geuns RJ *et al.* Quantification of left ventricular volumes and function in patients with cardiomyopathies by real-time three-dimensional echocardiography: a head-to-head comparison between two different semiautomated endocardial border detection algorithms. *J Am Soc Echocardiogr* 2007;**20**:1042–9.
18. Chukwu EO, Barasch E, Mihalatos DG, Katz A, Lachmann J, Han J *et al.* Relative importance of errors in left ventricular quantitation by two-dimensional echocardiography: insights from three-dimensional echocardiography and cardiac magnetic resonance imaging. *J Am Soc Echocardiogr* 2008;**21**:990–7.
19. Gopal AS, Chukwu EO, Iwuchukwu CJ, Katz AS, Toole RS, Schapiro W *et al.* Normal values of right ventricular size and function by real-time 3-dimensional echocardiography: comparison with cardiac magnetic resonance imaging. *J Am Soc Echocardiogr* 2007;**20**:445–55.
20. Mor-Avi V, Sugeng L, Weinert L, MacEneaney P, Caiani EG, Koch R *et al.* Fast measurement of left ventricular mass with real-time three-dimensional echocardiography, comparison with magnetic resonance imaging. *Circulation* 2004;**110**:1814–8.
21. Jacobs LD, Salgo IS, Goonewardena S, Weinert L, Coon P, Bardo D *et al.* Rapid online quantification of left ventricular volume from real-time three-dimensional echocardiographic data. *Eur Heart J* 2006;**27**:460–8.
22. Hansegård J, Urheim S, Lunde K, Malm S, Rabben SI. Semi-automated quantification of left ventricular volumes and ejection fraction by real-time three-dimensional echocardiography. *Cardiovasc Ultrasound* 2009;**7**:18.
23. Papademetris X, Sinusas AJ, Dione DP, Duncan JS. Estimation of 3D left ventricular deformation from echocardiography. *Med Image Anal* 2001;**5**:17–28.
24. Zhu Y, Papademetris X, Sinusas A, Duncan JS. Segmentation of myocardial volumes from real-time 3D echocardiography using an incompressibility constraint. *Proc Med Image Comput Comput Assist Interv* 2007;**LNCS 4791**:44–51.
25. Boukerroui D, Basset O, Baskurt A, Gimenez G. A multiparametric and multiresolution segmentation algorithm of 3-D ultrasonic data. *IEEE Trans Ultrason Ferroelectr Freq Control* 2001;**48**:64–77.
26. Ye X, Noble JA, Atkinson D. 3-D freehand echocardiography for automatic left ventricle reconstruction and analysis based on multiple acoustic windows. *IEEE Trans Med Imaging* 2002;**21**:1051–8.
27. Sanchez-Ortiz GI, Wright GJT, Clarke N, Declerck J, Banning AP, Noble JA. Automated 3-D echocardiography analysis compared with manual delineations and SPECT MUGA. *IEEE Trans Med Imaging* 2002;**21**:1069–76.
28. Angelini ED, Homma S, Pearson G, Holmes JW, Laine AF. Segmentation of real-time three-dimensional ultrasound for quantification of ventricular function: a clinical study on right and left ventricles. *Ultrasound Med Biol* 2005;**31**:1143–58.
29. Corsi C, Saracino G, Sarti A, Lamberti C. Left ventricular volume estimation for real-time three-dimensional echocardiography. *IEEE Trans Med Imaging* 2002;**21**:1202–8.
30. Lin N, Yu W, Duncan JS. Combinative multi-scale level set framework for echocardiographic image segmentation. *Med Image Anal* 2003;**7**:529–37.
31. Sarti A, Corsi C, Mazzini E, Lamberti C. Maximum likelihood segmentation of ultrasound images with Rayleigh distribution. *IEEE Trans Ultrason Ferroelectr Freq Control* 2005;**52**:947–60.
32. Caiani EG, Corsi C, Zamorano J, Sugeng L, MacEneaney P, Weinert L *et al.* Improved semiautomated quantification of left ventricular volumes and ejection fraction using 3-dimensional echocardiography with a full matrix-array transducer: comparison with magnetic resonance imaging. *J Am Soc Echocardiogr* 2005;**18**:779–88.
33. Bosch JG, Mitchell SC, Lelieveldt BPF, Nijland F, Kamp O, Sonka M *et al.* Automatic segmentation of echocardiographic sequences by active appearance motion models. *IEEE Trans Med Imaging* 2002;**21**:1374–83.
34. Ma M, Van Stralen M, Reiber JHC, Bosch JG, Lelieveldt BPF. Model driven quantification of left ventricular function from sparse single-beat 3D echocardiography. *Proc SPIE Med Imaging* 2009;**7259**:725907.
35. Hansegård J, Orderud F, Rabben SI. Real-time active shape models for segmentation of 3D cardiac ultrasound. *Proc Comput Anal Images Patterns* 2007;**LNCS 4673**:157–64.
36. Ma M, Van Stralen M, Reiber JHC, Bosch JG, Lelieveldt BPF. Left ventricle segmentation from contrast enhanced fast rotating ultrasound images using three dimensional active shape models. *Proc Func Imaging Modeling Heart* 2009;**LNCS 5528**:295–302.
37. Hansegård J, Urheim S, Lunde K, Rabben SI. Constrained active appearance models for segmentation of triplane echocardiograms. *IEEE Trans Med Imaging* 2007;**26**:1391–400.
38. Leung KYE, Van Stralen M, Voormolen MM, De Jong N, Van der Steen AFW, Reiber JHC *et al.* Improving 3D active appearance model segmentation of the left ventricle with jacobian tuning. *Proc SPIE Med Imaging* 2008;**6914**:69143B.
39. Van Stralen M, Leung KYE, Voormolen MM, De Jong N, Van der Steen AFW, Reiber JHC *et al.* Automatic segmentation of the left ventricle in 3D echocardiography using active appearance models. *Proc Int Ultrason Symp* 2007;**1**:1480–3.
40. Coppini G, Poli R, Valli G. Recovery of the 3-D shape of the left ventricle from echocardiographic images. *IEEE Trans Med Imaging* 1995;**14**:301–17.
41. Georgescu B, Zhou XS, Comaniciu D, Gupta A. Database-guided segmentation of anatomical structures with complex appearance. *Proc Comput Vis Pattern Recogn* 2005;**2**:429–36.
42. Lu X, Georgescu B, Zheng Y, Otsuki J, Comaniciu D. Autompr: automatic detection of standard planes in 3D echocardiography. *Proc Int Symp Biomed Imaging* 2008;**1**:1279–82.
43. Georgescu B. Whitepaper: automated volumetric cardiac ultrasound analysis. 2008. http://www.medicalsiemenscom/siemens/en_US/gg_us_FBAs/files/misc_downloads/Whitepaper_Georgescupdf.
44. Yang L, Georgescu B, Zheng Y, Foran DJ, Comaniciu D. A fast and accurate tracking algorithm of left ventricles in 3D echocardiography. *Proc Int Symp Biomed Imaging* 2008;**1**:221–4.
45. Leung KYE, Danilouchkine MG, Van Stralen M, De Jong N, Van der Steen AFW, Bosch JG. Tracking left ventricular borders in 3D echocardiographic sequences using motion-guided optical flow. *Proc SPIE Med Imaging* 2009;**7259**:72590W.
46. Myronenko A, Song X, Sahn DJ. LV motion tracking from 3D echocardiography using textural and structural information. *Proc Med Image Comput Comput Assist Interv* 2007;**10**:428–35.
47. Elen A, Choi HF, Loeckx D, Gao H, Claus P, Suetens P *et al.* Three-dimensional cardiac strain estimation using spatio-temporal elastic registration of ultrasound images: a feasibility study. *IEEE Trans Med Imaging* 2008;**27**:1580–91.
48. Veronesi F, Corsi C, Caiani EG, Sarti A, Lamberti C. Tracking of left ventricular long axis from real-time three-dimensional echocardiography using optical flow techniques. *IEEE Trans Inf Technol Biomed* 2006;**10**:174–81.
49. Linguraru MG, Vasilyev NV, Marx GR, Tworetzky W, Del Nido PJ, Howe RD. Fast block flow tracking of atrial septal defects in {4D} echocardiography. *Med Image Anal* 2008;**12**:397–412.
50. Kawagishi T. Speckle tracking for assessment of cardiac motion and dyssynchrony. *Echocardiography* 2008;**25**:1167–71.
51. Nesser HJ, Winter S. Speckle tracking in the evaluation of left ventricular dyssynchrony. *Echocardiography* 2009;**26**:324–36.
52. Perez de Isla L, Balcones DV, Fernandez-Golfin C, Marcos-Alberca P, Almeria C, Rodrigo JL *et al.* Three-dimensional-wall motion tracking: a new and faster tool for myocardial strain assessment: comparison with two-dimensional-wall motion tracking. *J Am Soc Echocardiogr* 2009;**22**:325–30.
53. Duan Q, Angelini ED, Herz SL, Ingrassia CM, Costa KD, Holmes JW *et al.* Region-based endocardium tracking on real-time three-dimensional ultrasound. *Ultrasound Med Biol* 2009;**35**:256–265.
54. Mor-Avi V, Jenkins C, Kuhl HP, Nesser HJ, Marwick T, Franke A *et al.* Real-time 3-dimensional echocardiographic quantification of left ventricular volumes: multicenter study for validation with magnetic resonance imaging and investigation of sources of error. *JACC Cardiovasc Imaging* 2008;**1**:413–23.
55. Nikitin NP, Constantin C, Loh PH, Ghosh J, Lukaschuk EI, Bennett A *et al.* New generation 3-dimensional echocardiography for left ventricular volumetric and functional measurements: comparison with cardiac magnetic resonance. *Eur J Echocardiogr* 2006;**7**:365–72.
56. Jenkins C, Chan J, Hanekom L, Marwick T. Accuracy and feasibility of online 3-dimensional echocardiography for measurement of left ventricular parameters. *J Am Soc Echocardiogr* 2006;**19**:1119–28.
57. Sugeng L, Mor-Avi V, Weinert L, Niel J, Ebner C, Steringer-Mascherbauer R *et al.* Quantitative assessment of left ventricular size and function: side-by-side comparison of real-time three-dimensional echocardiography and computed tomography with magnetic resonance reference. *Circulation* 2006;**114**:654–61.
58. Riehle TJ, Mahle WT, Parks WJ, Sallee D 3rd, Fyfe DA. Real-time three-dimensional echocardiographic acquisition and quantification of left ventricular indices in children and young adults with congenital heart disease: comparison with magnetic resonance imaging. *J Am Soc Echocardiogr* 2008;**21**:78–83.
59. Heimann T, van Ginneken B, Styner MA, Arzhaeva Y, Aurich V, Bauer C *et al.* Comparison and evaluation of methods for liver segmentation from CT datasets. *IEEE Trans Med Imaging* 2009;**28**:1251–65.

60. Ecabert O, Peters J, Schramm H, Lorenz C, von Berg J, Walker MJ *et al.* Automatic model-based segmentation of the heart in CT images. *IEEE Trans Med Imaging* 2008;**27**:1189–201.
61. Nillesen MM, Lopata RGP, de Boode W, Kapusta L, Huisman HJ, Thijssen JM *et al.* 3D cardiac segmentation using temporal correlation of radiofrequency ultrasound data. *Proc Med Image Comput Comput Assist Interv* 2008;**LNCS 5762**:927–934.
62. Orderud F, Rabben SI. Real-time 3D segmentation of the left ventricle using deformable subdivision surfaces. *Proc Comput Vis Pattern Recogn* 2008;**1**:1–8.
63. Caiani EG, Sugeng L, Weinert L, Capderou A, Lang RM, Vaida P. Objective evaluation of changes in left ventricular and atrial volumes during parabolic flight using real-time three-dimensional echocardiography. *J Appl Physiol* 2006;**101**:460–8.
64. Chan J, Jenkins C, Khafagi F, Du L, Marwick TH. What is the optimal clinical technique for measurement of left ventricular volume after myocardial infarction? A comparative study of 3-dimensional echocardiography, single photon emission computed tomography, and cardiac magnetic resonance imaging. *J Am Soc Echocardiogr* 2006;**19**:192–201.
65. Jenkins C, Bricknell K, Hanekom L, Marwick TH. Reproducibility and accuracy of echocardiographic measurements of left ventricular parameters using real-time three-dimensional echocardiography. *J Am Coll Cardiol* 2004;**44**:878–86.
66. Jenkins C, Leano R, Chan J, Marwick TH. Reconstructed versus real-time 3-dimensional echocardiography: comparison with magnetic resonance imaging. *J Am Soc Echocardiogr* 2007;**20**:862–8.
67. Burgess MI, Jenkins C, Chan J, Marwick TH. Measurement of left ventricular dyssynchrony in patients with ischaemic cardiomyopathy: a comparison of real-time three-dimensional and tissue Doppler echocardiography. *Heart* 2007;**93**:1191–6.
68. van der Heide JA, Mannaerts HF, Spruijt HJ, van Campen LM, de Cock C, Visser CA *et al.* Noninvasive mapping of left ventricular electromechanical asynchrony by three-dimensional echocardiography and semi-automatic contour detection. *Am J Cardiol* 2004;**94**:1449–53.
69. Kapetanakis S, Kearney MT, Siva A, Gall N, Cooklin M, Monaghan MJ. Real-time three-dimensional echocardiography: a novel technique to quantify global left ventricular mechanical dyssynchrony. *Circulation* 2005;**112**:992–1000.
70. Jenkins C, Bricknell K, Chan J, Hanekom L, Marwick TH. Comparison of two- and three-dimensional echocardiography with sequential magnetic resonance imaging for evaluating left ventricular volume and ejection fraction over time in patients with healed myocardial infarction. *Am J Cardiol* 2007;**99**:300–6.
71. Soliman OI, Krenning BJ, Geleijnse ML, Nemes A, van Geuns RJ, Baks T *et al.* A comparison between qlab and tomtec full volume reconstruction for real time three-dimensional echocardiographic quantification of left ventricular volumes. *Echocardiography* 2007;**24**:967–74.
72. van Dijk J, Knaapen P, Russel IK, Hendriks T, Allaart CP, de Cock CC *et al.* Mechanical dyssynchrony by 3D echo correlates with acute haemodynamic response to biventricular pacing in heart failure patients. *Europace* 2008;**10**:63–8.
73. Liang XC, Cheung EW, Wong SJ, Cheung YF. Impact of right ventricular volume overload on three-dimensional global left ventricular mechanical dyssynchrony after surgical repair of tetralogy of fallot. *Am J Cardiol* 2008;**102**:1731–6.
74. Niemann PS, Pinho L, Balbach T, Galuschky C, Blankenhagen M, Silberbach M *et al.* Anatomically oriented right ventricular volume measurements with dynamic three-dimensional echocardiography validated by 3-tesla magnetic resonance imaging. *J Am Coll Cardiol* 2007;**50**:1668–76.
75. Horton KD, Meece RW, Hill JC. Assessment of the right ventricle by echocardiography: a primer for cardiac sonographers. *J Am Soc Echocardiogr* 2009;**22**:776–92.
76. Tamborini G, Brusoni D, Torres Molina JE, Galli CA, Maltagliati A, Muratori M *et al.* Feasibility of a new generation three-dimensional echocardiography for right ventricular volumetric and functional measurements. *Am J Cardiol* 2008; **102**:499–505.
77. Takeuchi M, Jacobs A, Sugeng L, Nishikage T, Nakai H, Weinert L *et al.* Assessment of left ventricular dyssynchrony with real-time 3-dimensional echocardiography: comparison with doppler tissue imaging. *J Am Soc Echocardiogr* 2007;**20**: 1321–9.
78. Kleijn SA, van Dijk J, de Cock CC, Allaart CP, van Rossum AC, Kamp O. Assessment of intraventricular mechanical dyssynchrony and prediction of response to cardiac resynchronization therapy: comparison between tissue Doppler imaging and real-time three-dimensional echocardiography. *J Am Soc Echocardiogr* 2009; **22**:1047–1054.
79. Takeuchi M, Nishikage T, Mor-Avi V, Sugeng L, Weinert L, Nakai H *et al.* Measurement of left ventricular mass by real-time three-dimensional echocardiography: validation against magnetic resonance and comparison with two-dimensional and m-mode measurements. *J Am Soc Echocardiogr* 2008;**21**:1001–5.
80. Anwar AM, Soliman OI, Geleijnse ML, Nemes A, Vletter WB, ten Cate FJ. Assessment of left atrial volume and function by real-time three-dimensional echocardiography. *Int J Cardiol* 2008;**123**:155–61.
81. Artang R, Migrino RQ, Harmann L, Bowers M, Woods TD. Left atrial volume measurement with automated border detection by 3-dimensional echocardiography: comparison with magnetic resonance imaging. *Cardiovasc Ultrasound* 2009; **7**:16.
82. Walimbe V, Garcia M, Lalude O, Thomas J, Shekhar R. Quantitative real-time 3-dimensional stress echocardiography: a preliminary investigation of feasibility and effectiveness. *J Am Soc Echocardiogr* 2007;**20**:13–22.
83. van Stralen M, Bosch JG, Voormolen MM, van Burken G, Krenning BJ, van Geuns RM *et al.* Left ventricular volume estimation in cardiac three-dimensional ultrasound: a semiautomatic border detection approach. *Acad Radiol* 2005;**12**: 1241–9.
84. Yan P, Sinusas A, Duncan JS. Boundary element method-based regularization for recovering of LV deformation. *Med Image Anal* 2007;**11**:540–54.
85. Caiani EG, Corsi C, Sugeng L, MacEneaney P, Weinert L, Mor-Avi V *et al.* Improved quantification of left ventricular mass based on endocardial and epicardial surface detection with real time three dimensional echocardiography. *Heart* 2006;**92**:213–9.
86. Song M, Haralick RM, Sheehan FH, Johnson RK. Integrated surface model optimization for freehand three-dimensional echocardiography. *IEEE Trans Med Imaging* 2002;**21**:1077–90.
87. Yu W, Yan P, Sinusas AJ, Thiele K, Duncan JS. Towards pointwise motion tracking in echocardiographic image sequences—comparing the reliability of different features for speckle tracking. *Med Image Anal* 2006;**10**:495–508.